

# BotGraph: Large Scale Spamming Botnet Detection

Yao Zhao<sup>†</sup>, \*Yinglian Xie, Fang Yu, Qifa Ke, Yuan Yu, Yan Chen<sup>†</sup>, and Eliot Gillum<sup>‡</sup>

<sup>†</sup>Northwestern University

Microsoft Research Silicon Valley

<sup>‡</sup>Microsoft Corporation

## Abstract

Network security applications often require analyzing huge volumes of data to identify abnormal patterns or activities. The emergence of cloud-computing models opens up new opportunities to address this challenge by leveraging the power of parallel computing.

In this paper, we design and implement a novel system called *BotGraph* to detect a new type of botnet spamming attacks targeting major Web email providers. BotGraph uncovers the correlations among botnet activities by constructing large user-user graphs and looking for tightly connected subgraph components. This enables us to identify stealthy botnet users that are hard to detect when viewed in isolation. To deal with the huge data volume, we implement BotGraph as a distributed application on a computer cluster, and explore a number of performance optimization techniques. Applying it to two months of Hotmail log containing over 500 million users, BotGraph successfully identified over 26 million botnet-created user accounts with a low false positive rate. The running time of constructing and analyzing a 220GB Hotmail log is around 1.5 hours with 240 machines. We believe both our graph-based approach and our implementations are generally applicable to a wide class of security applications for analyzing large datasets.

## 1 Introduction

Despite a significant breadth of research into botnet detection and defense (e.g., [8, 9]), botnet attacks remain a serious problem in the Internet today and the phenomenon is evolving rapidly ([4, 5, 9, 20]): attackers constantly craft new types of attacks with an increased level of sophistication to hide each individual bot identities.

One recent such attack is the *Web-account abuse attack* [25]. Its large scale and severe impact have repeatedly caught public media's attention. In this attack, spammers use botnet hosts to sign up millions of user accounts (denoted as *bot-users* or *bot-accounts*) from major free Web email service providers such as AOL, Gmail, Hotmail, and Yahoo!Email. The numerous abused bot-accounts were used to send out billions of spam emails across the world.

Existing detection and defense mechanisms are ineffective against this new attack: The widely used mail server reputation-based approach is not applicable because bot-users send spam emails through only legitimate

Web email providers. Furthermore, it is difficult to differentiate a bot-user from a legitimate user individually, as both users may share a common computer and that each bot-user sends only a few spam emails<sup>1</sup>.

While detecting bot-users individually is difficult, detecting them as an aggregate holds the promise. The rationale is that since bot-users are often configured similarly and controlled by a small number of botnet commanders, they tend to share common features and correlate each other in their behavior such as active time, spam contents, or email sending strategies [24, 27]. Although this approach is appealing, realizing it to enable detection at a large scale has two key challenges:

- The first is the algorithmic challenge in finding subtle correlations among bot-user activities and distinguishing them from normal user behavior.
- The second challenge is how to efficiently analyze a large volume of data to unveil the correlations among hundreds of millions of users. This requires processing hundreds of gigabytes or terabytes of user activity logs.

Recent advancement in distributed programming models, such as MapReduce [6], Hadoop [2], and Dryad/DryadLINQ [10, 29], has made programming and computation on a large distributed cluster much easier. This provides us with opportunities to leverage the parallel computing power to process data in a scalable fashion. However, there still exist many system design and implementation choices.

In this paper, we design and implement a system called *BotGraph* to detect the Web-account abuse attack at a large scale. We make two important contributions.

Our first contribution is to propose a novel graph-based approach to detect the new Web-account abuse attack. This approach exposes the underlying correlations among user-login activities by constructing a *large user-user graph*. Our approach is based on the observation that bot-users *share IP addresses* when they log in and send emails. BotGraph detects the abnormal sharing of IP addresses among bot-users by leveraging the random graph theory. Applying BotGraph to two months of Hotmail log of total 450GB data, BotGraph successfully identified over 26 million bot-accounts with a low false positive rate of 0.44%. To our knowledge, we are the first to provide a

<sup>1</sup>Recent anecdotal evidence suggests that bot-users have also been programmed to receive emails and read them to make them look more legitimate.

\*The work was done while Yao was an intern at Microsoft Research Silicon Valley.

systematic solution that can successfully detect this new large-scale attack.

Our second contribution is an efficient implementation using the new distributed programming models for constructing and analyzing large graphs. In our application, the graph to construct involves tens of millions of nodes and hundreds of billions of edges. It is challenging to efficiently construct such large graphs on a computer cluster as the task requires computing pair-wise correlations between any two users. We present two graph construction methods using different execution plans: the simpler one is based on the MapReduce model [6], and the other performs selective filtering that requires the Join operation provided by Map-Reduce-Merge [28] or DryadLINQ [29]. By further exploring several performance optimization strategies, our implementation can process a one-month dataset (220GB-240GB) to construct a large graph with tens of millions of nodes in 1.5 hours using a 240-machine cluster. The ability to efficiently compute large graphs is critical to perform constant monitoring of user-user graphs for detecting attacks at their earliest stage.

Our ultimate goal, however, is not to just tackle this specific new form of attacks, but also to provide a general framework that can be adapted to other attack scenarios. To this end, the adoption of a graph representation can potentially enable us to model the correlations of a wide class of botnet attacks using various features. Furthermore, since graphs are powerful representations in many tasks such as social network analysis and Web graph mining, we hope our large-scale implementations can serve as an example to benefit a wide class of applications for efficiently constructing and analyzing large graphs.

The rest of the paper is organized as follows. We discuss related work in Section 2, and overview the BotGraph system in Section 3. We then describe in Section 4 the detail algorithms to construct and analyze a large user-user graph for attack detection. We present the system implementation and performance evaluation in Section 5, followed by attack detection results in Section 6. Finally, we discuss attacker countermeasures and system generalizations in Section 7.

## 2 Background and Related Work

In this section, we first describe the new attack we focus on in our study, and review related work in botnet detection and defense. As we use Dryad/DryadLINQ as our programming model for analyzing large datasets, we also discuss existing approaches for parallel computation on computer clusters, particularly those relate to the recent cloud computing systems.

### 2.1 Spamming Botnets and Their Detection

The recent Web-account abuse attack was first reported in summer 2007 [25], in which millions of botnet email accounts were created from major Web email service providers in a short duration for sending spam emails.

While each user is required to solve a CAPTCHA test to create an account, attackers have found ways to bypass CAPTCHAs, for example, redirecting them to either spammer-controlled Web sites or dedicated cheap labor<sup>2</sup>. The solutions are sent back to the bot hosts for completing the automated account creation. Trojan.Spammer.HotLan is a typical worm for such automated account signup [25]. Today, this attack is one of the major types of large-scale botnet attacks, and many large Web email service providers, such as Hotmail, Yahoo!Mail, and Gmail, are the popular attack targets. To our best knowledge, BotGraph is one of the first solutions to combat this new attack.

The Web-account abuse attack is certainly not the first type of botnet spamming attacks. Botnet has been frequently used as a media for setting up spam email servers. For example, a backdoor rootkit Spam-Mailbot.c can be used to control the compromised bots to send spam emails. Storm botnet, one of the most widespread P2P botnets with millions of hosts, at its peak, was deemed responsible for generating 99% of all spam messages seen by a large service provider [9, 19].

Although our work primarily focuses on detecting the Web-account abuse attack, it can potentially be generalized to detect other botnet spamming attacks. In this general problem space, a number of previous studies have all provided us with insights and valuable understanding towards the different characteristics of botnet spamming activities [1, 11, 23, 26]. Among recent work on detecting botnet membership [20, 22, 24, 27], SpamTracker [24] and AutoRE [27] also aim at identifying correlated spamming activities and are more closely related with our work. In addition to exploiting common features of botnet attacks as SpamTracker and AutoRE do, BotGraph also leverages the connectivity structures of the user-user relationship graph and explores these structures for botnet account detection.

### 2.2 Distributed and Parallel Computing

There has been decades of research on distributed and parallel computing. Massive parallel processing (MPP) develops special computer systems for parallel computing [15]. Projects such as MPI (Message Passing Interface) [14] and PVM(Parallel Virtual Machine) [21] develop software libraries to support parallel computing. Distributed database is another large category of parallel data processing applications [17].

The emergence of cloud computing models, such as MapReduce [6], Hadoop [2], Dryad/DryadLINQ [10, 29], has enabled us to write simple programs for efficiently analyzing a vast amount of data on a computer cluster. All of them adopt the notion of staged computation, which makes scheduling, load balancing, and failure recovery automatic. This opens up a plethora of opportunities for re-thinking network security—an application

<sup>2</sup>Interestingly, solving CAPTCHAs has ended up being a low-wage industry [3].

that often requires processing huge volumes of logs or trace data. Our work is one of the early attempts in this direction.

While all of these recent parallel computing models offer scalability to distributed applications, they differ in programming interfaces and the built-in operation primitives. In particular, MapReduce and Hadoop provide two simple functions, Map and Reduce, to facilitate data partitioning and aggregation. This abstraction enables applications to run computation on multiple data partitions in parallel, but is difficult to support other common data operations such as database Join. To overcome this shortcoming, Map-Reduce-Merge [28] introduces a Merge phase to facilitate the joining of multiple heterogeneous datasets. More recent scripting languages, such as Pig Latin [16] and Sawzall [18], wrap the low level MapReduce procedures and provide high-level SQL-like query interfaces. Microsoft Dryad/DryadLINQ [10, 29] offers further flexibility. It allows a programmer to write a simple C# and LINQ program to realize a large class of computation that can be represented as a DAG.

Among these choices, we implemented BotGraph using Dryad/DryadLINQ, but we also consider our processing flow design using the more widely used MapReduce model and compare the pros and cons. In contrast to many other data-centric applications such as sorting and histogram computation, it is much more challenging to decompose graph construction for parallel computation in an efficient manner. In this space, BotGraph serves as an example system to achieve this goal using the new distributed computing paradigm.

### 3 BotGraph System Overview

Our goal is to capture spamming email accounts used by botnets. As shown in Figure 1, BotGraph has two components: aggressive sign-up detection and stealthy bot-user detection. Since service providers such as Hotmail limit the number of emails an account can send in one day, a spammer would try to sign up as many accounts as possible. So the first step of BotGraph is to detect aggressive *signups*. The purpose is to limit the total number of accounts owned by a spammer. As a second step, BotGraph detects the remaining stealthy bot-users based on their *login* activities. With the total number of accounts limited by the first step, spammers have to reuse their accounts, resulting in correlations among account logins. Therefore BotGraph utilizes a graph based approach to identify such correlations. Next, we discuss each component in detail.

#### 3.1 Detection of Aggressive Signups

Our aggressive signup detection is based on the premise that signup events happen infrequently at a single IP address. Even for a proxy, the number of users signed up from it should be roughly consistent over time. A sudden increase of signup activities is suspicious, indicating that the IP address may be associated with a bot. We use

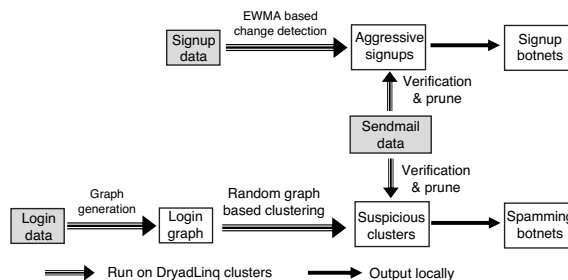


Figure 1: The Architecture of BotGraph.

a simple EWMA (Exponentially Weighted Moving Average) [13] algorithm to detect sudden changes in signup activities. This method can effectively detect over 20 million bot-users in 2 months (see Appendix A for more details on EWMA). We can then apply adaptive throttling to rate limit account-signup activities from the corresponding suspicious IP addresses.

One might think that spammers can gradually build up an aggressive signup history for an IP address to evade EWMA-based detection. In practice, building such a history requires a spammer to have full control of the IP address for a long duration, which is usually infeasible as end-users control the online/offline switch patterns of their (compromised) computers. The other way to evade EWMA-based detection is to be stealthy. In the next section we will introduce a graph based approach to detect stealthy bot-users.

#### 3.2 Detection of Stealthy Bot-accounts

Our second component detects the remaining stealthy bot-accounts. As a spammer usually controls a set of bot-users, defined as a *bot-user group*, these bot-users work in a collaborative way. They may share similar login or email sending patterns because bot-masters often manage all their bot-users using unified toolkits. We leverage the similarity of bot-user behavior to build a user-user graph. In this graph, each vertex is a user. The weight for an edge between two vertices is determined by the features we use to measure the similarity between the two vertices (users). By selecting the appropriate features for similarity measurement, a bot-user group will reveal itself as a connected component in the graph.

In BotGraph, we use the number of common IP addresses logged in by two users as our similarity feature (i.e., edge weight). This is because the aggressive account-signup detection limits the number of bot-accounts a spammer may obtain. In order to achieve a large spam-email throughout, each bot-account will log in and send emails multiple times at different locations, resulting in the sharing of IP addresses as explained below:

- **The sharing of one IP address:** For each spammer, the number of bot-users is typically much larger than the number of bots. Our data analysis shows that on each day, the average number of bot-users is about

50 times more than the number of bots. So multiple bot-users must log in from a common bot, resulting in the sharing of a common IP address.

- **The sharing of multiple IP addresses:** We found that botnets may have a high churn rate. A bot may be quarantined and leave the botnet, and new bots may be added. An active bot may go offline and it is hard to predict when it will come back online. To maximize the bot-account utilization, each account needs to be assigned to different bots over time. Thus a group of bot-accounts will also share multiple IP addresses with a high probability.

Our BotGraph system leverages the two aforementioned IP sharing patterns to detect bot-user activities.

Note that with dynamic IP addresses and proxies, normal users may share IP addresses too. To exclude such cases, multiple shared IP addresses in the same Autonomous System (AS) are only counted as one shared IP address. In the rest of this paper, we use the number of “shared IP addresses” to denote the the number of ASes of the shared IP addresses. It is very rare to have a group of normal users that always coincidentally use the same set of IP addresses across different domains. Using the AS-number metric, a legitimate user on a compromised bot will not be mistakenly classified as a bot-user because their number of “shared IPs” will be only one<sup>3</sup>.

## 4 Graph-Based Bot-User Detection

In this section we introduce random graph models to analyze the user-user graph. We show that bot-user groups differentiate themselves from normal user groups by forming giant components in the graph. Based on the model, we design a hierarchical algorithm to extract such components formed by bot-users. Our overall algorithm consists of two stages: 1) constructing a large user-user graph, 2) analyzing the constructed graph to identify bot-user groups. Note one philosophy we use is to analyze group properties instead of single account properties. For example, it may be difficult to use email-sending statistics for individual bot-account detection (each bot account may send a few emails only), but it is very effective to use the group statistics to estimate how likely a group of accounts are bot-accounts (e.g., they all sent a similar number of emails).

### 4.1 Modeling the User-User Graph

The user-user graph formed by bot-users is drastically different from the graph formed by normal users: bot-users have a higher chance of sharing IP addresses and thus more tightly connected in the graph. Specifically, we observed the bot-user subgraph contains a *giant connected component*—a group of connected vertices that occupies a significant portion of the subgraph, while

<sup>3</sup>We assume majority of hosts are physically located in only one AS. We discuss how to prune legitimate mobile users in Section 4.2.2.

the normal-user subgraph contains only isolated vertices and/or very small connected components. We introduce the random graph theory to interpret this phenomenon and to model the giant connected components formed by bot-users. The theory also serves as a guideline for designing our graph-based bot-user detection algorithm.

#### 4.1.1 Giant Component in User-User Graph

Let us first consider the following three typical strategies used by spammers for assigning bot-accounts to bots, and examine the corresponding user-user graphs.

- Bot-user accounts are randomly assigned to bots. Obviously, all the bot-user pairs have the same probability  $p$  to be connected by an edge.
- The spammer keeps a queue of bot-users (i.e., the spammer maintains all the bot-users in a predefined order). The bots come online in a random order. Upon request from a bot when it comes online, the spammer assigns to the requesting bot the top  $k$  available (currently not used) bot-users in the queue. To be stealthy, a bot makes only one request for  $k$  bot-users each day.
- The third case is similar to the second case, except that there is no limit on the number of bot-users a bot can request for one day and that  $k = 1$ . Specifically, a bot requests one bot-account each time, and it asks for another account after finishing sending enough spam emails using the current account.

We simulate the above typical spamming strategies and construct the corresponding user-user graph. In the simulation, we have 10,000 spamming accounts ( $n = 10,000$ ) and 500 bots in the botnet. We assume all the bots are active for 10 days and the bots do not change IP addresses. In model 2, we pick  $k = 20$ . In model 3, we assume the bots go online with a Poisson arrival distribution and the length of bot online time fits a exponential distribution. We run each simulation setup 10 times and present the average results.

Figure 2 shows the simulation results. We can see that there is a sharp increase of the size of the largest connected component as the threshold  $T$  decreases (i.e., the probability of two vertices being connected increases). In other words, there exists some transition point of  $T$ . If  $T$  is above this transition point, the graph contains only isolated vertices and/or small components. Once  $T$  crosses the transition point, the giant component “suddenly” appears. Note that different spamming strategies may lead to different transition values. Model 2 has a transition value of  $T = 2$ , while Model 1 and 3 have the same transition value of  $T = 3$ .

Using email server logs and a set of known botnet accounts provided by the Hotmail operational group, we have confirmed that generally bot-users are above the transition point of forming giant components, while normal users usually cannot form large components with more than 100 nodes.



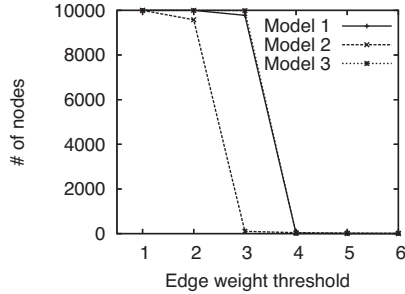


Figure 2: The size of the largest connected component.

#### 4.1.2 Random Graph Theory

The sudden appearance of a giant subgraph component after a transition point can be interpreted by the theory of random graphs.

Denote  $G(n, p)$  as the random graph model, which generates a  $n$ -vertex graph by simply assigning an edge to each pair of vertices with probability  $p \in (0, 1]$ . We call the generated graph an instance of the model  $G(n, p)$ . The parameter  $p$  determines when a giant connected component will appear in the graph generated by  $G(n, p)$ . The following property is derived from theorems in [7, p.65~67]:

**Theorem 1** *A graph generated by  $G(n, p)$  has average degree  $d = n \cdot p$ . If  $d < 1$ , then with high probability the largest component in the graph has size less than  $O(\log n)$ . If  $d > 1$ , with high probability the graph will contain a giant component with size at the order of  $O(n)$ .*

For a group of bot-users that share a set of IPs, the average degree will be larger than one. According to the above theorem, the giant component will appear with a high probability. On the other hand, normal users rarely share IPs, and the average degree will be far less than one when the number of vertices is large. The resulted graph of normal users will therefore contain isolated vertices and/or small components, as we observe in our case. In other words, the theorem interprets the appearance of giant components we have observed in subsection 4.1.1. Based on the theorem, the sizes of the components can serve as guidelines for bot-user pruning and grouping (discussed in subsection 4.2.2 and 4.2.3).

#### 4.2 Bot-User Detection Algorithm

As we have shown in section 4.1, a bot-user group forms a connected component in the user-user graph. Intuitively one could identify bot-user groups by simply extracting the connected components from the user-user graph generated with some predefined threshold  $T$  (the least number of shared IPs for two vertices to be connected by an edge). In reality, however, we need to handle the following issues:

- It is hard to choose a single fixed threshold of  $T$ . As we can see from Figure 2, different spamming strategies may lead to different transition points.

- Bot-users from different bot-user groups may be in the same connected component. This happens due to: 1) bot-users may be shared by different spammers, and 2) a bot may be controlled by different spammers.
- There may exist connected components of normal users. For example, mobile device users roaming around different locations will be assigned IP addresses from different ASs, and therefore appeared as a connected component.

To handle these problems, we propose a hierarchical algorithm to extract connected components, followed by a pruning and grouping procedure to remove false positives and to separate mixed bot-user groups.

#### 4.2.1 Hierarchical Connected-Component Extraction

Algorithm 1 describes a recursive function Group\_Extracting that extracts a set of connected components from a user-user graph in a hierarchical way. Having such a recursive process avoids using a fixed threshold  $T$ , and is potentially robust to different spamming strategies.

Using the original user-user graph as input, Bot-Graph begins with applying Group\_Extracting( $G, T$ ) to the graph with  $T = 2$ . In other words, the algorithm first identifies all the connected components with edge weight  $w \geq 2$ . It then recursively increases  $w$  to extract connected subcomponents. This recursive process continues until the number of nodes in the connected component is smaller than a pre-set threshold  $M$  ( $M = 100$  in our experiments). The final output of the algorithm is a hierarchical tree of the connected components with different edge weights.

```

procedure Group_Extracting( $G, T$ )
1 Remove all the edges with weight  $w < T$  from  $G$ 
  and suppose we get  $G'$ ;
2 Find out all the connected subgraphs  $G_1, G_2, \dots,$ 
   $G_k$  in  $G'$ ;
3 for  $i = 1 : k$  do
4   | Let  $|G_k|$  be the number of nodes in  $G_k$ ;
5   | if  $|G_k| > M$  then
6   |   | Output  $G_k$  as a child node of  $G$ ;
7   |   | Group_Extracting( $G_k, T + 1$ );
   | end
3 end

```

**Algorithm 1:** A Hierarchical algorithm for connected component extraction from a user-user graph.

#### 4.2.2 Bot-User Pruning

For each connected component output by Algorithm 1, we want to compute the level of confidence that the set of users in the component are indeed bot-users. In particular, we need to remove from the tree (output by Al-

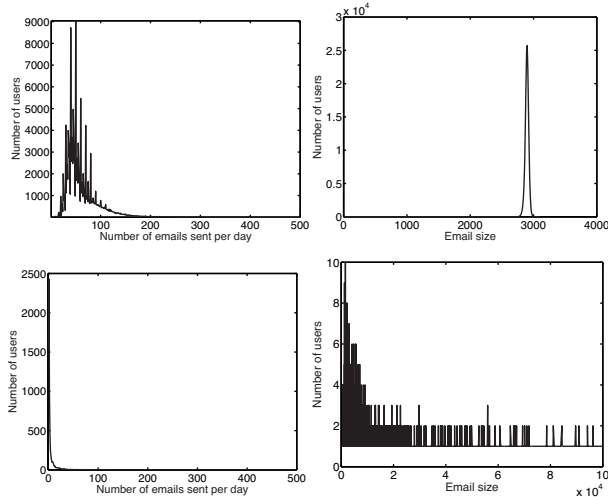


Figure 3: Histograms of (1) number of emails sent per day and (2) email size. First row: aggressive bot-users; second row: normal users.

gorithm 1) the connected components involving mostly legitimate/normal users.

A major difference between normal users and bot-users is the way they send emails. More specifically, normal users usually send a small number of emails per day on average, with different email sizes. On the other hand, bot-users usually send many emails per day, with identical or similar email sizes, as they often use a common template to generate spam emails. It may be difficult to use such differences in email-sending statistics to classify bot-accounts individually. But when a group of accounts are viewed in aggregate, we can use these statistics to estimate how likely the entire group are bot-users. To do so, for each component, BotGraph computes two histograms from a 30-day email log:

- $h_1$ : the numbers of emails sent per day per user.
- $h_2$ : the sizes of emails.

Figure 3 shows two examples of the above two histograms, one computed from a component consisting of bot-users (the first row), the other from a component of normal users (the second row). The distributions are clearly different. Bot-users in a component sent out a larger number of emails on average, with similar email sizes (around 3K bytes) that are visualized as the peak in the email-size histogram. Most normal users sent a small number of emails per day on average, with email sizes distributing more uniformly. BotGraph normalizes each histogram such that its sum equals to one, and computes two statistics,  $s_1$  and  $s_2$ , from the normalized histograms to quantify their differences:

- $s_1$ : the percentage of users who sent more than 3 emails per day;
- $s_2$ : the areas of peaks in the normalized email-size histogram, or the percentage of users who sent out emails with a similar size.

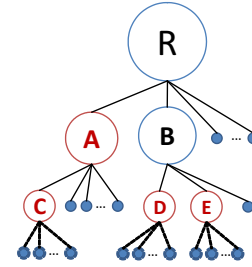


Figure 4: An example of extracting bot-user groups using the random graph model.

Since the histograms are normalized, both  $s_1$  and  $s_2$  are in the range of  $[0, 1]$  and can be used as confidence measures. A large confidence value means that the majority of the users in the connected component are bot-users. We use only  $s_1$  to choose the candidates of bot-user components, because  $s_1$  represents a more robust feature. We use  $s_2$  together with other features (e.g., account naming patterns) for validation purpose only (see Section 6).

In the pruning process, BotGraph traverses the tree output by Algorithm 1. For each node in the tree, it computes  $s_1$ , the confidence measure for this node to be a bot-user component, and removes the node if  $s_1$  is smaller than a threshold  $S$ . In total, fewer than 10% of Hotmail accounts sent more than 3 emails per day, so intuitively, we can set the threshold  $S = 0.1$ . In order to minimize the number of false positive users, we conservatively set the threshold  $S = 0.8$ , i.e., we only consider nodes where at least 80% of users sent more than 3 emails per day as suspicious bot-user groups (discussed further in Section 6.2).

#### 4.2.3 Bot-User Grouping

After pruning, a candidate connected-component may contain two or more bot-user groups. BotGraph proceeds to decompose such components further into individual bot-user groups. The correct grouping is important for two reasons:

- We can extract validation features (e.g.,  $s_2$  mentioned above and patterns of account names) more accurately from individual bot-user groups than from a mixture of different bot-user groups.
- Administrators may want to investigate and take different actions on different bot-user groups based on their behavior.

We use the random graph model to guide the process of selecting the correct bot-user groups. According to the random graph model, the user-user subgraph of a bot-user group should consist of a giant connected-component plus very small components and/or isolated vertices. So BotGraph traverses the tree again to select tree nodes that are consistent with such random graph property. For each node  $V$  being traversed, there are two cases:

- $V$ 's children contain one or more giant components whose sizes are  $O(N)$ , where  $N$  is the number of users in node  $V$ ;

- $V$ 's children contain only isolated vertices and/or small components with size of  $O(\log(N))$ .

For case 1, we recursively traverse each subtree rooted by the giant components. For case 2, we stop traversing the subtree rooted at the  $V$ . Figure 4 illustrates the process. Here the root node  $R$  is decomposed into two giant components  $A$  and  $B$ .  $B$  is further decomposed into another two giant components  $D$  and  $E$ , while  $A$  is decomposed into one giant component  $C$ . The giant component disappears for any further decomposition, indicated by the dash-lines. According to the theory,  $A$ ,  $C$ ,  $D$ , and  $E$  are bot-user groups. If a node is chosen as a bot-user group, the sub-tree rooted at the chosen node is considered belonging to the same bot-user group. That is, if we pick  $A$ , we disregard its child  $C$  as it is a subcomponent of  $A$ .

## 5 Large-scale Parallel Graph Construction

The major challenge in applying BotGraph is the construction of a large user-user graph from the Hotmail login data – the first stage of our graph-based analysis described in Section 3.2. Each record in the input log data contains three fields: *UserID*, *IPAddress*, and *Login-Timestamp*. The output of the graph construction is a list of edges in the form of  $UserID_1$ ,  $UserID_2$ , and *Weight*. The number of users on the graph is over 500 million based on a month-long login data (220 GB), and this number is increasing as the Hotmail user population is growing. The number of edges of the computed graph is on the order of hundreds of billions. Constructing such a large graph using a single computer is impractical. An efficient, scalable solution is required so that we could detect attacks as early as possible in order to take timely reactive measures.

For data scalability, fault tolerance, and ease of programming, we choose to implement BotGraph using Dryad/DryadLINQ, a powerful programming environment for distributed data-parallel computing. However, constructing a large user-user graph using Dryad/DryadLINQ is non-trivial. This is because the resulting graph is extremely *large*, therefore a straightforward parallel implementation is inefficient in performance. In this section, we discuss in detail our solutions. We first present both a simple parallelism method and a selective filtering method, and then describe several optimization strategies and their performance impacts. We also discuss several important issues arising in the system implementation, such as data partitioning, data processing flow, and communication methods. Using a one-month log as input, our current implementation can construct a graph with tens of millions of nodes in 1.5 hours using a 240-machine cluster. During this process, BotGraph filters out weight one edges, and the remaining number of edges for the next-stage processing is around 8.6 billion.

We also implemented the second stage of finding connected components using Dryad/DryadLINQ. This stage can be solved using a divide and conquer algorithm. In

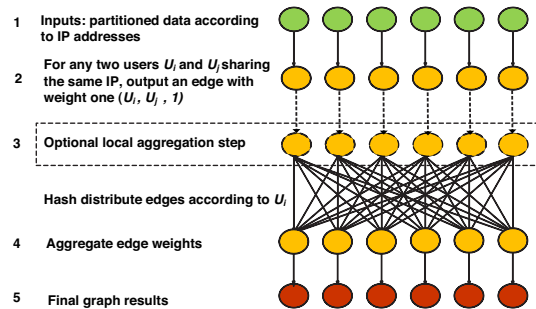


Figure 5: Process flow of Method 1.

particular, one can divide the graph edges into multiple partitions, identify the connected subgraph components in each partition, and then merge the incomplete subgraphs iteratively. To avoid overloading the merging node, instead of sending all outputs to a single merging node, each time we merge two results from two partitions. This parallel algorithm is both efficient and scalable. Using the same 240-machine cluster in our experiments, this parallel algorithm can analyze a graph with 8.6 billion edges in only 7 minutes — 34 times faster than the 4 hour running time by a single computer. Given our performance bottleneck is at the first stage of graph construction instead of graph analysis, we do not further elaborate this step.

### 5.1 Two Implementation Methods

The first step in data-parallel applications is to partition data. Based on the ways we partition the input data, we have different data processing flows in implementing graph construction.

#### 5.1.1 Method 1: Simple Data Parallelism

Our first approach is to partition data according to IP address, and then to leverage the well known Map and Reduce operations to straightforwardly convert graph construction into a data-parallel application.

As illustrated in Figure 5, the input dataset is partitioned by the user-login IP address (Step 1). During the Map phase (Step 2 and 3), for any two users  $U_i$  and  $U_j$  sharing the same IP-day pair, where the IP address is from Autonomous System  $AS_k$ , we output an edge with weight one  $e = (U_i, U_j, AS_k)$ . Only edges pertaining to different ASes need to be returned (Step 3). To avoid outputting the same edge multiple times, we use a local hash table to filter duplicate edges.

After the Map phase, all the generated edges (from all partitions) will serve as inputs to the Reduce phase. In particular, all edges will be hash partitioned to a set of processing nodes for weight aggregation using  $(U_i, U_j)$  tuples as hash keys (Step 4). Obviously, for those user pairs that only share one IP-day in the entire dataset, there is only one edge between them. So no aggregation can be performed for these weight one edges. We will show later in Figure 7 that weight one edges are the dominate source of graph edges. Since BotGraph focuses on only

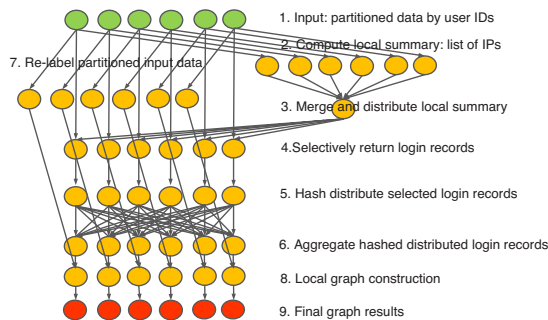


Figure 6: Process flow of Method 2.

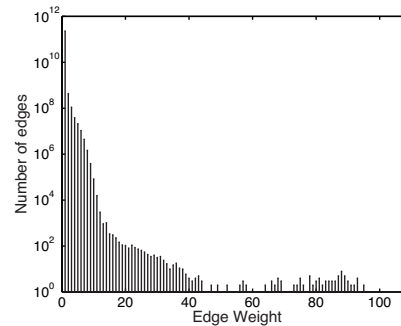


Figure 7: Edge weight distribution.

edges with weight two and above, the weight one edges introduce unnecessary communication and computation cost to the system. After aggregation, the outputs of the Reduce phase are graph edges with aggregated weights.

### 5.1.2 Method 2: Selective Filtering

An alternative approach is to partition the inputs based on user ID. In this way, for any two users that were located in the same partition, we can directly compare their lists of IP-day pairs to compute their edge weight. For two users whose records locate at different partitions, we need to ship one user's records to another user's partition before computing their edge weight, resulting in huge communication costs.

We notice that for users who do not share any IP-day keys, such communication costs can be avoided. That is, we can reduce the communication overhead by *selectively filtering* data and distributing only the related records across partitions.

Figure 6 shows the processing flow of generating user-user graph edges with such an optimization. For each partition  $p_i$ , the system computes a *local summary*  $s_i$  to represent the union of all the IP-day keys involved in this partition (Step 2). Each local summary  $s_i$  is then distributed across all nodes for selecting the relevant input records (Step 3). At each partition  $p_j (j \neq i)$ , upon receiving  $s_i$ ,  $p_j$  will return all the login records of users who shared the same IP-day keys in  $s_i$ . This step can be further optimized based on the edge threshold  $w$ : if a user in  $p_j$  shares fewer than  $w$  IP-day keys with the summary  $s_i$ , this user will not generate edges with weight at least  $w$ . Thus only the login records of users who share at least  $w$  IP-day keys with  $s_i$  should be selected and sent to partition  $p_i$  (Step 4). To ensure the selected user records will be shipped to the right original partition, we add an additional label to each original record to denote their partition ID (Step 7). Finally, after partition  $p_i$  receives the records from partition  $p_j$ , it joins these remote records with its local records to generate graph edges (Step 8 and 9).

Other than Map and Reduce, this method requires two additional programming interface supports: the operation to join two heterogeneous data streams and the operation to broadcast a data stream.

### 5.1.3 Comparison of the Two Methods

In general, Method 1 is simple and easy to implement, but Method 2 is more optimized for our application. The main difference between the two data processing flows is that Method 1 generates edges of weight one and sends them across the network in the Reduce phase, while Method 2 directly computes edges with weight  $w$  or more, with the overhead of building a local summary and transferring the selected records across partitions. Figure 7 shows the distribution of edge weights using one-month of user login records as input. Here, the number of weight one edges is almost three orders of magnitude more than the weight two edges. In our botnet detection, we are interested in edges with a minimum weight two because weight one edges do not show strong correlated login activities between two users. Therefore the computation and communication spent on generating weight one edges are not necessary. Although in Method 1, Step 3 can perform local aggregation to reduce the number of duplicated weight one edges, local aggregation does not help much as the number of unique weight one edges dominates in this case.

Given our implementation is based on the existing distributed computing models such as MapReduce and DryadLINQ, the amount of intermediate results impacts the performance significantly because these programming models all adopt disk read/write as cross-node communication channels. Using disk access as communication is robust to failures and easy to restart jobs [6, 29]. However, when the communication cost is large such as in our case, it becomes a major bottleneck of the overall system running time. To reduce this cost, we used a few optimization strategies and will discuss them in the next subsection. Completely re-designing or customizing the underlying communication channels may improve the performance in our application, but is beyond the scope of this paper.

Note the amount of cross-node communication also depends on the cluster size. Method 1 results in a constant communication overhead, i.e., the whole edge set, regardless of the number of data partitions. But for Method 2, when the number of computers (hence the number of data partitions) increases, both the aggregated local summary size and the number of user-records to be shipped



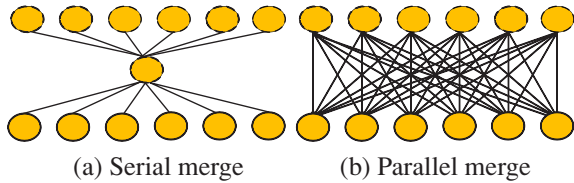


Figure 8: (a) Default query execution plan (b) Optimized query execution plan.

increase, resulting in a larger communication overhead. In the next subsections, we present our implementations and evaluate the two different methods using real-data experiments.

## 5.2 Implementations and Optimizations

In our implementation, we have access to a 240-machine cluster. Each machine is configured with an AMD Dual Core 4.3G CPU and 16 GB memory. As a pre-processing step, all the input login records were hash partitioned evenly to the computer cluster using the DryadLINQ built-in hash-partition function.

Given the Hotmail login data is on the order of hundreds of Gigabytes, we spent a number of engineering efforts to reduce the input data size and cross-node communication costs. The first two data reduction strategies can be applied to both methods. The last optimization is customized for Method 2 only.

**1. User pre-filtering:** We pre-filter users by their login AS numbers: if a user has logged in from IP addresses across multiple ASes in a month, we regard this user as a suspicious user candidate. By choosing only suspicious users (using 2 ASes as the current threshold) and their records as input, we can reduce the number of users to consider from over 500 million (about 200-240GB) to about 70 million (about 100GB). This step completes in about 1-2 minutes.

**2. Compression:** Given the potential large communication costs, BotGraph adopts the DryadLINQ provided compression option to reduce the intermediate result size. The use of compression can reduce the amount of cross-node communication by 2-2.5 times.

**3. Parallel data merge:** In Method 2, Step 3 merges the local IP-day summaries generated from every node and then broadcasts the aggregated summary to the entire cluster. The old query plan generated by DryadLINQ is shown in Figure 8 (a), where there exists a single node that performs data aggregation and distribution. In our experiments, this aggregating node becomes a big bottleneck, especially for a large cluster. So we modified DryadLINQ to generate a new query plan that supports parallel data aggregation and distribution from every processing node (Figure 8 (b)). We will show in Section 5.3 that this optimization can reduce the broadcast time by 4-5 times.

	Communication data size	Total running time
Method 1	12.0 TB	> 6 hours
Method 2	1.7 TB	95 min

Table 1: Performance comparison of the two methods using the 2008-dataset.

	Communication data size	Total running time
Method 1 (no comp.)	2.71 TB	135 min
Method 1 (with comp.)	1.02 TB	116 min
Method 2 (no comp.)	460 GB	28 min
Method 2 (with comp.)	181 GB	21 min

Table 2: Performance comparison of the two methods using a subset of the 2008-dataset.

## 5.3 Performance Evaluation

In this section, we evaluate the performance of our implementations using a one-month Hotmail user-login log collected in Jan 2008 (referred to as the 2008-dataset). The raw input data size is 221.5 GB, and after pre-filtering, the amount of input data is reduced to 102.9 GB. To use all the 240 machines in the cluster, we generated 960 partitions to serve as inputs to Method 1 (so that the computation of each partition fits into memory), and generated 240 partitions as inputs to Method 2. With compression and parallel data merge both enabled, our implementation of Method 2 finishes in about 1.5 hours using all the 240 machines, while Method 1 cannot finish within the maximum 6 hour quota allowed by the computer cluster (Table 1). The majority of time in Method 1 is spent on the second Reduce step to aggregate a huge volume of intermediate results. For Method 2, the local summary selection step generated about 5.8 GB aggregated IP-day pairs to broadcast across the cluster, resulting 1.35 TB out of the 1.7 TB total traffic.

In order to benchmark performance, we take a smaller dataset (about 1/5 of the full 2008-dataset) that Method 1 can finish within 6 hours. Table 2 shows the communication costs and the total running time using the 240 machine cluster. While Method 1 potentially has a better scalability than Method 2 as discussed in Section 5.1.3, given our practical constraints on the cluster size, Method 2 generates a smaller amount of traffic and outperforms Method 1 by about 5-6 times faster. The use of compression reduces the amount of traffic by about 2-3 times, and the total running time is about 14-25% faster.

To evaluate the system scalability of Method 2, we vary the number of data partitions to use different number of computers. Figure 9 shows how the communication overheads grow. With more partitions, the amount of data generated from each processing node slightly decreases, but the aggregated local summary data size increases (Figure 9 (a)). This is because popular IP-day pairs may appear in multiple data partitions and hence in the aggregated summary multiple times. Similarly, the same user login records will also be shipped across a larger number of nodes, increasing the communication

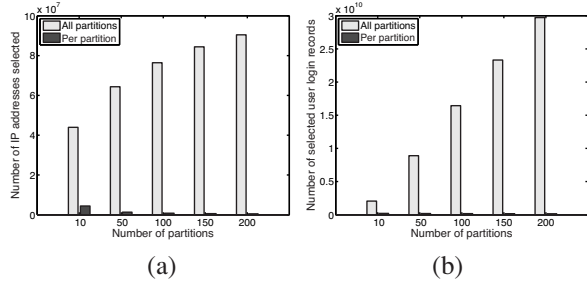


Figure 9: Communication data size as we vary the number of input data partitions (a) Local summary size in terms of the number of IP-day keys. (b) Total number of selected user login records to be sent across the network.

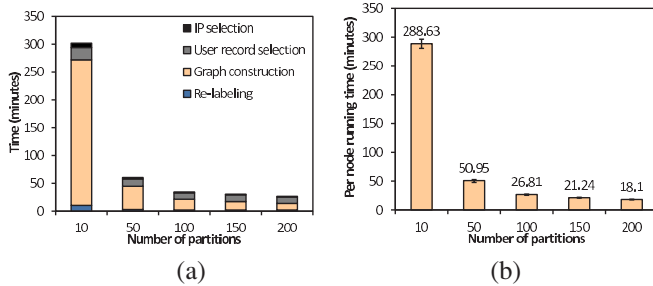


Figure 10: Running time as we vary the number of input data partitions for Method 2. (a) Total running time of all partitions. (b) The running of each partition. The error bars show the max and the min running time across all partitions.

costs as the system scales (Figure 9 (b)).

Even though the communication costs increase, the total running time is still reduced with a larger cluster size. Figure 10 (a) shows the total running time and its breakdown across different steps. When the cluster size is small (10 partitions), a dominant amount of time is spent on computing the graph edges. As the system scales, this portion of time decreases sharply. The other three steps are I/O and network intensive. Their running time slightly decreases as we increase the number of partitions, but the savings get diminished due to the larger communication costs. Figure 10 (b) shows the average running time spent on processing each partition, and its variations are very small.

We now examine the benefits of adopting parallel data merge. The purpose of parallel data merge is to remove the bottleneck node that performs data aggregation and broadcasting. Since it is difficult to factor out the network transfer time savings alone (network, disk I/O, and computation are pipelined), we compare the time spent on the user record selection step (Figure 11 (a)). This optimization can reduce the processing latency significantly as the cluster size increases (75% reduction in the 200 node scenario). Without parallel data merge, the processing time increases almost linearly, but with this optimization, the amount of time remains roughly constant.

For Method 2, one reason for the large communication costs is that for botnet users, their graph component

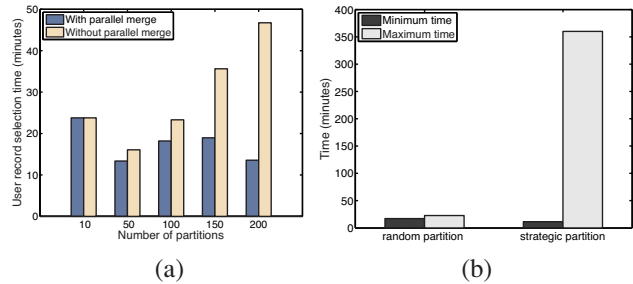


Figure 11: (a) The processing time of user-record selection with and without parallel data merge. (b) Minimal and maximum running time of partitions with and without strategic data partitioning.

is both large and dense. Therefore, one potential optimization technique is to strategically partition the login records. Intuitively, we can reduce the communication costs if we pre-group users so that users who are heavily connected are placed in one partition, and users who are placed in different partitions have very few edges between them. If so, Step 4 in Method 2 will return only a small number of records to ship across different nodes. Surprisingly, we found this strategy actually induced negative impact on the system performance.

Figure 11 (b) shows the graph construction time spent at a processing node with and without strategic data partitioning. We chose the 240 input data partition scenario and use the full dataset to illustrate the performance difference. In the first case, we evenly distributed login records by hashing user IDs. In the second case, we chose a large botnet user group with 3.6M users and put all their login records evenly across 5 partitions, with the remaining data evenly distributing across the remaining partitions. This scenario assumes the best prior knowledge of user connections. Although in both cases, the total amount of input data in each partition is roughly uniform, we observe a big difference between the maximum and minimum time in computing the edges across nodes. Without strategic partitioning, the maximum and minimum processing time is very close. In contrast, strategic partitioning caused a huge degree of unbalance in workload, resulting in much longer total job running time.

## 6 Bot-user Detection and Validation

We use two month-long datasets as inputs to our system: a 2007-dataset collected in Jun 2007, and a 2008-dataset collected in Jan 2008. Each dataset includes two logs: a Hotmail login log (format described in Section 5) and a Hotmail signup log. Each record in the signup log contains a user-ID, the remote IP address used for signup, and the signup timestamp. For each dataset, we run our EWMA-based anomaly detection on the signup log and run our graph based detection on the login log. Using both components, BotGraph detected tens of millions of bot users and millions of botnet IPs. Table 3 summarizes the results for both months. We present the detailed results and perform evaluations next.

Month	06/2007	01/2008
# of bot-users	5.97M	20.58M
# of bot-IPs	2.71M	1.84M

Table 3: Total bot-users and bot IP addresses detected using both history based detection and user-user graph.

Month	06/2007	01/2008
# of bot IPs	82,026	240,784
# of bot-user accounts	4.83 M	16.41 M
Avg. anomaly window	1.45 day	1.01 day

Table 4: History based detection of bot IP addresses and bot-user accounts.

Month	06/2007	01/2008
# of bot-groups	13	40
# of bot-accounts	2.66M	8.68M
# of unique IPs	2.69M	1.60M

Table 5: Bot IP addresses and bot-user accounts detected by user-user graphs.

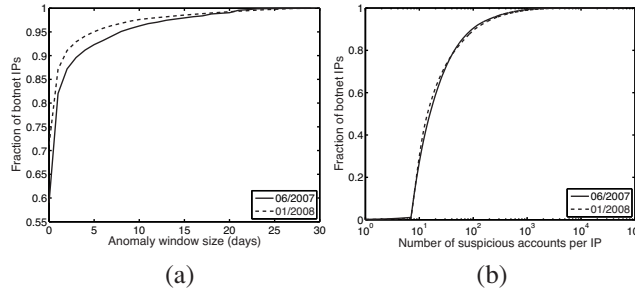


Figure 12: (a) Cumulative distribution of anomaly window size in terms of number of days. (b) Cumulative distribution of the number of accounts signed up per suspicious IP.

### 6.1 Detection Using Signup History

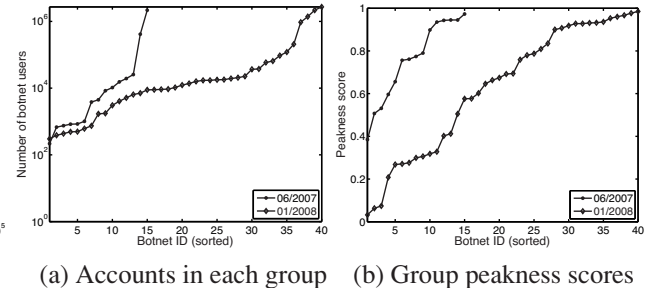
Table 4 shows that the EWMA algorithm detected 21.2 million bot-user accounts when applied to the two Hotmail signup logs. Comparing Jan 2008 with Jun 2007, both the number of bot IPs and the signed-up bot-users increased significantly. In particular, the total number of bot-accounts signed up in Jan 2008 is more than three times the number in Jun 2007. Meanwhile, the anomaly window is shortened from an average of 1.45 days to 1.01 days, suggesting each attack became shorter in Jan 2008.

Figure 12 (a) shows the cumulative distribution of the anomaly window sizes associated with each bot IP address. A majority (80% - 85%) of the detected IP addresses have small anomaly windows, ranging from a few hours to one day, suggesting that many botnet signup attacks happened in a burst.

Figure 12 (b) shows the cumulative distributions of the number of accounts signed up per bot IP. As we can see, the majority of bot IPs signed up a large number of accounts, even though most of them have short anomaly windows. Interestingly, the cumulative distributions derived from Jun 2007 and Jan 2008 overlap well with each other, although we observed a much larger number of bot IPs and bot-users in Jan 2008. This indicates that the overall bot-user signup activity patterns still remain similar perhaps due to the reuse of bot-account signup tools/software.

### 6.2 Detection by User-User Graph

We apply the graph-based bot-user detection algorithm on the Hotmail login log to derive a tree of connected components. Each connected component is a set of bot-user candidates. We then use the procedures described in Section 4.2.2 to prune the connected components of normal users. Recall that in the pruning process, we apply a threshold on the confidence measure of each component (computed from the “email-per-day” feature) to re-



(a) Accounts in each group (b) Group peakness scores

Figure 13: Bot-user group properties: (a) The the number of users per group, (b) The peakness score of each group, reflecting whether there exists a strong sharp peak for the email size distribution.

move normal user components. In our experiments, the confidence measures are well separated: most of the bot-groups have confidence measures close to 1, and a few groups are between 0.4 and 0.6. We observe a wide margin around confidence measure of 0.8, which we choose as our threshold. As discussed in Section 4.2.2, this is a conservative threshold and is in-sensitive to noises due to the wide margin. For any group that has a confidence measure below 0.8, we regard it as a normal user group and prune it from our tree.

Table 5 shows the final detection results after pruning and grouping. Both the number of bot-users and the number of bot IP addresses are on the order of millions — a non-trivial fraction of all the users and IP addresses observed by Hotmail. We find the two sets of bot-users detected in two months hardly overlap. These accounts were stealthy ones, each sending out only a few to tens of spam emails during the entire month. Therefore, it is difficult to capture them by looking for aggressive sending patterns. Due to their large population, detecting and sanitizing these users are important both to save Hotmail resources and to reduce the amount of spam sent to the Internet. Comparing Jan 2008 with Jun 2007, the number of bot-users tripled, suggesting that using Web portals as a spamming media has become more popular.

Now we study the properties of bot-users at a group level. Figure 13 (a) shows that the number of users in each group ranges from thousands to millions. Comparing Jan 2008 with Jun 2007, although the largest bot-user group remains similar in size, the number of groups increased significantly. This confirms our previous observation that spammers are more frequently using Web email accounts for spam email attacks.

We next investigate the email sending patterns of the detected bot user groups. We are interested in whether there exists a strong peak of email sizes. We use the peak-

ness score metric  $s_2$  (defined in Section 4.2.2) to quantify the degree of email size similarity for each group. Figure 13 (b) shows the distributions of  $s_2$  in sorted order. A majority of groups have peakness scores higher than 0.6, meaning that over 60% of their emails have similar sizes. For the remaining groups, we performed manual investigation and found they have multiple peaks, resulting in lower scores. The similarity of their email sizes is a strong evidence of correlated email sending activities.

In the next two sub-sections, we explore the quality of the total captured 26 million bot-users. First, we examine whether they are known bad and how many of them are our new findings. Second, we estimate our detection false positive rates.

### 6.3 Known Bot-users vs. New Findings

We evaluate our detected bot-users against a set of known spammer users reported by other email servers in Jan 2008<sup>4</sup>.

Denote  $H$  as the set of bot-users detected by signup history using EWMA,  $K_s$  as the set of known spammer accounts signed up in the month that we study, and  $K_s \cap H$  as the intersection between  $H$  and  $K_s$ . The ratio of  $\frac{K_s \cap H}{H}$  represents the percentage of captured bot-users that are previously known bad. In other words,  $1 - \frac{K_s \cap H}{H}$  is our new findings. The ratio of  $\frac{K_s \cap H}{K_s}$  denotes the recall of our approach. Table 6 shows that, in Jun 2007, 85.15% of the EWMA-detected bot-user detected are already known bad, and the detected bot-user covers a significant fraction of bad account, i.e., recall = 67.96%. Interestingly, Jan 2008 yields quite different results. EWMA is still able to detect a large fraction of known bad account. However, only 8.17% of detected bad-users were reported to be bad. That means 91.83% of the captured spamming accounts are our new findings.

We apply a similar study to the bot-users detected by the user-user graph. Denote  $K_l$  as the set of known spammers users that log in from at least 2 ASes,  $L$  as the set of bot-users detected using our user-user graph based approach, and  $K_l \cap L$  as the intersect between  $K_l$  and  $L$ . Again we use the ratios of  $\frac{K_l \cap L}{L}$  and  $\frac{K_l \cap L}{K_l}$  to evaluate our result  $L$ , as shown in Table 7. Using our graph-based approach, the recall is higher. In total, we were able to detect 76.84% and 85.80% of known spammer users in Jun 2007 and Jan 2008, respectively. Similar to EWMA, the graph-based detection also identified a large number (54.10%) of previously unknown bot-accounts in Jan 2008. This might be because these accounts are new ones and haven't been used aggressively to send out a massive amount of spam emails yet. So, they are not yet reported by other mail servers as of Jan 2008. The ability of detecting bot-accounts at an early stage is important to give us an upper hand in the anti-spam battle.

<sup>4</sup>These users were complained of having sent outbound spam emails.

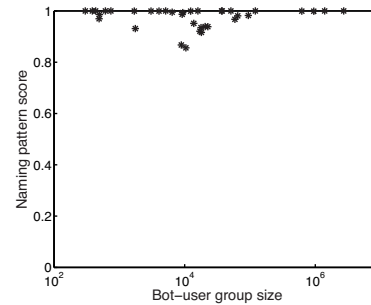


Figure 14: Validation of login-graph detected bot-users using naming scores.

### 6.4 False Positive Analysis

In the previous subsection, we analyzed the overlap between our results and the set of known bad accounts. For the remaining ones, validation is a challenging task without the ground truth. We examine the following two account features to estimate the false positive rates: naming patterns and signup dates.

#### 6.4.1 Naming Patterns

For the identified groups, we found almost every group follows a very clear user-name template, for example, a fixed-length sequence of alphabets mixed with digits<sup>5</sup>. Examples of such names are “w9168d4dc8c5c25f9” and “x9550a21da4e456a2”.

To quantify the similarity of account names in a group, we introduce a *naming pattern score*, which is defined as the largest fraction of users that follow a single template. Each template is a regular expression derived by a regular expression generation tool [27]. Since many accounts detected in Jun 2007 were known bad and hence cleaned by the system already, we focus on bot-user groups detected in Jan 2008.

Figure 14 shows the naming score distribution. A majority of the bot-user groups have close to 1 naming pattern scores, indicating that they were signed up by spammers using some fixed templates. There are only a few bot-user groups with scores lower than 0.95. We manually looked at them and found that they are also bad users, but the user names come from two naming templates. It is possible that our graph-based approach mixed two groups, or the spammers purchased two groups of bot-users and used them together. Overall, we found in total only 0.44% of the identified bot-users do not strictly follow the naming templates of their corresponding groups.

#### 6.4.2 Signup Dates

Our second false positive estimate is based on examining the signup dates of the detected bot-users. Since the Web-account abuse attack is recent and started in summer 2007, we regard all the accounts signed up before 2007 as legitimate accounts. Only 0.08% of the identified bot-users were signed up before year 2007. To cal-

<sup>5</sup>Note it is hard to directly use the naming pattern itself to identify spamming accounts due to the easy countermeasures.



$I = K_s \cap H$	06/2007	01/2008
$I/H$	85.15%	8.17%
$I/K_s$	67.96%	52.41%

Table 6: Comparing bot-users detected by signup history using EWMA with known spammer user sets, using the ratios of  $\frac{K_s \cap H}{H}$  and  $\frac{K_s \cap H}{K_s}$ . See text for the definition of  $H$  and  $K_s$ .

ibrate our results against the entire user population. We look at the sign up dates of all users in the input dataset. About 59.1% of the population were signed up before 2007. Assuming the normal user signup-date distributions are the same among the overall population and our detected user set, we adjust the false positive rate to be  $0.08\%/59.1\% = 0.13\%$

The above two estimations suggest that the false positive of BotGraph is low. We conservatively pick the higher one 0.44% as our false positive rate estimate.

## 7 Discussion

In this paper, we demonstrated that BotGraph can detect tens of millions of bot-users and millions of bots. With this information, operators can take remedy actions and mitigate the ongoing attacks. For bot-users, operators can block their accounts to prevent them from further sending spam, or apply more strict policies when they log in (e.g., request them to do additional CAPTCHA tests). For detected bot IP addresses, one approach is to blacklist them or rate limit their login activities, depending on whether the corresponding IP address is a dynamically assigned address or not. Effectively throttling botnet attacks in the existence of dynamic IP addresses is ongoing work.

Attackers may wish to evade the BotGraph detection by developing countermeasures. For example, they may reduce the number of users signed up by each bot. They may also mimic the normal user email-sending behavior by reducing the number of emails sent per account per day (e.g., fewer than 3). Although mimicking normal user behavior may evade history-based change detection or our current thresholds, these approaches also significantly limit the attack scale by reducing the number of bot-accounts they can obtain or the total number of spam emails to send. Furthermore, BotGraph can still capture the graph structures of bot-user groups from their login activity to detect them.

A more sophisticated evasion approach may bind each bot-user to only bots in one AS, so that our current implementation would pre-filter them by the two AS threshold. To mitigate this attack, BotGraph may revise the edge weight definition to look at the number of IP prefixes instead of the number of ASes. This potentially pushes the attacker countermeasures to be more like a fixed IP-account binding strategy. As discussed in Section 3.2, binding each bot-user to a fixed bot is not desirable to the spammers. Due to the high botnet churn rate, it would result in a low bot-user utilization rate. It also makes attack detection easier by having a fixed group of aggressive accounts on the same IP addresses all the

$I = K_l \cap L$	06/2007	01/2008
$I/L$	90.95%	45.9%
$I/K_l$	76.84%	85.8%

Table 7: Comparing bot-users detected by user-user graph with known spammer user sets, using the ratios of  $\frac{K_l \cap L}{L}$  and  $\frac{K_l \cap L}{K_l}$ . See text for the definition of  $K_l$  and  $L$ .

time. If one of the bot-accounts is captured, the entire group can be easily revealed. A more generalized solution is to broaden our edge weight definition by considering additional feature correlations. For example, we can potentially use email sending patterns such as the destination domain [24], email size, or email content patterns (e.g., URL signatures [27]). As ongoing work, we are exploring a larger set of features for more robust attack detection.

In addition to using graphs, we may also consider other alternatives to capture the correlated user activity. For example, we may cluster user accounts using their login IP addresses as feature dimensions. Given the large data volume, how to accurately and efficiently cluster user accounts into individual bot-groups remains a challenging research problem.

It is worth mentioning that the design and implementation of BotGraph can be applied in different areas for constructing and analyzing graphs. For example, in social network studies, one may want to group users based on their buddy relationship (e.g., from MSN or Yahoo messengers) and identify community patterns. Finally, although our current implementations are Dryad/DryadLINQ specific, we believe the data processing flows we propose can be potentially generalized to other programming models.

## 8 Conclusion

We designed and implemented *BotGraph* for Web mail service providers to defend against botnet launched Web-account abuse attacks. BotGraph consists of two components: a history-based change-detection component to identify aggressive account signup activities and a graph-based component to detect stealthy bot-user login activities. Using two-month Hotmail logs, *BotGraph* successfully detected more than 26 million botnet accounts. To process a large volume of Hotmail data, BotGraph is implemented as a parallel Dryad/DryadLINQ application running on a large-scale computer cluster. In this paper, we described our implementations in detail and presented performance optimization strategies. As general-purpose distributed computing frameworks have become increasingly popular for processing large datasets, we believe our experience will be useful to a wide category of applications for constructing and analyzing large graphs.

## 9 Acknowledgement

We would like to thank Mihai Budiu, Úlfar Erlingsson, and Dennis Fetterly for their help on DryadLINQ. We are grateful to the Hotmail operation team for providing us

with data and valuable feedbacks. We would also like to thank Nick Feamster and anonymous reviewers for their constructive comments.

## A EWMA based Aggressive Signup Detection

Exponentially Weighted Moving Average (EWMA) is a well known moving average based algorithm to detect sudden changes. EWMA is both simple and effective, and has been widely used for anomaly detection [12].

Given a time series data, let the observation value at time  $t$  be  $Y_t$ . Let  $S_t$  be the predicted value at time  $t$  and  $\alpha$  ( $0 \leq \alpha \leq 1$ ) be the weighting factor, EWMA predicts  $S_t$  as

$$S_t = \alpha \times Y_{t-1} + (1 - \alpha) \times S_{t-1} \quad (1)$$

We define the absolute prediction error  $E_t$  and the relative prediction error  $R_t$  as:

$$E_t = Y_t - S_t, \quad R_t = Y_t / \max(S_t, \epsilon) \quad (2)$$

where  $\epsilon$  is introduced to avoid the divide-by-zero problem. A large prediction error  $E_t$  or  $R_t$  indicates a sudden change in the time series data and should raise an alarm. When the number of new users signed up has dropped to the number before the sudden change, the sudden change ends. We define the time window between the start and the end of a sudden change as *the anomaly window*. All the accounts signed up during this anomaly window are suspicious bot-users.

In our implementation, we consider the time unit of a day, and hence  $E_t$  is the predicted number of daily signup accounts. For any IP address, if both  $E_t > \delta_E$  and  $R_t > \delta_R$ , we mark day  $t$  as the start of its anomaly window. From a two-year Hotmail signup log, we derive the 99%-tile of the daily number of account signups per IP address. To be conservative, we set the threshold  $\delta_E$  to be twice this number to rule out non-proxy normal IPs. For proxies, the relative prediction error is usually a better metric to separate them from bots. It is very rare for a proxy to increase its signup volume by 4 times overnight. So we conservatively set  $\delta_R$  to 4.

## References

- [1] D. S. Anderson, C. Fleizach, S. Savage, and G. M. Voelker. Spamscatter: Characterizing internet scam hosting infrastructure. In *USENIX Security Symposium*, 2007.
- [2] Apache. Hadoop. <http://lucene.apache.org/hadoop/>.
- [3] <http://blogs.zdnet.com/security/?p=1835>.
- [4] K. Chiang and L. Lloyd. A case study of the rustock rootkit and spam bot. In *First workshop on hot topics in understanding botnets*, 2007.
- [5] N. Daswani, M. Stoppelman, the Google Click Quality, and S. Teams. The anatomy of Clickbot.A. In *First workshop on hot topics in understanding botnets*, 2007.
- [6] J. Dean and S. Ghemawat. MapReduce: Simplified data processing on large clusters. In *OSDI*, 2004.
- [7] R. Durrett. *Random graph dynamics*. Cambridge University Press, 2006.
- [8] G. Gu, J. Zhang, and W. Lee. Botsniffer: Detecting botnet command and control channels in network traffic. In *NDSS*, 2008.
- [9] T. Holz, M. Steiner, F. Dahl, E. W. Biersack, and F. Freiling. Measurements and mitigation of peer-to-peer-based botnets: A case study on storm worm. In *LEET*, 2008.
- [10] M. Isard, M. Budiu, Y. Yu, A. Birrell, and D. Fetterly. Dryad: Distributed data-parallel programs from sequential building blocks. In *EuroSys*, 2007.
- [11] C. Kanich, C. Kreibich, K. Levchenko, B. Enright, G. Voelker, V. Paxson, and S. Savage. Spamalytics: An empirical analysis of spam marketing conversion. In *ACM CCS*, 2008.
- [12] B. Krishnamurthy, S. Sen, Y. Zhang, and Y. Chen. Sketch-based change detection: Methods, evaluation, and applications. In *ACM SIGCOMM IMC*, 2003.
- [13] Moving average. [http://en.wikipedia.org/wiki/Moving\\_average](http://en.wikipedia.org/wiki/Moving_average).
- [14] Message passing interface. <http://www-unix.mcs.anl.gov/mpi/>.
- [15] Massive parallel processing. [http://en.wikipedia.org/wiki/Massive\\_parallelism](http://en.wikipedia.org/wiki/Massive_parallelism).
- [16] C. Olston, B. Reed, U. Srivastava, R. Kumar, and A. Tomkins. Pig latin: A not-so-foreign language for data processing. In *ACM SIGMOD*, 2008.
- [17] M. T. Ozsu and P. Valduriez. *Principles of Distributed Database Systems (2nd edition)*. Prentice-Hall, 1999.
- [18] R. Pike, S. Dorward, R. Griesemer, and S. Quinla. Interpreting the data: Parallel analysis with sawzall. *Scientific Programming Journal*, 13(4), 2005.
- [19] P. Porras, H. Saidi, and V. Yegneswaran. A multi-perspective analysis of the storm (peacomm) worm. Technical report, SRI Computer Science Laboratory, 2007.
- [20] H. Project and R. Alliance. Know your enemy: Tracking botnets. <http://www.honeynet.org/papers/bots/>, 2005.
- [21] Parallel virtual machine. <http://www.csm.ornl.gov/pvm/>.
- [22] M. A. Rajab, J. Zarfoss, F. Monroe, and A. Terzis. A multifaceted approach to understanding the botnet phenomenon. In *IMC*, 2006.
- [23] A. Ramachandran and N. Feamster. Understanding the network-level behavior of spammers. In *ACM SIGCOMM*, 2006.
- [24] A. Ramachandran, N. Feamster, and S. Vempala. Filtering spam with behavioral blacklisting. In *ACM CCS*, 2007.
- [25] <http://news.bitdefender.com/NW544-en-\\--Trojan-Now-Uses-Hotmail-Gmail-as\\-Spam-Hosts.html>.
- [26] Y. Xie, F. Yu, K. Achan, E. Gillum, M. Goldszmidt, and T. Wobber. How dynamic are ip addresses? In *ACM SIGCOMM*, 2007.
- [27] Y. Xie, F. Yu, K. Achan, R. Panigrahy, G. Hulten, and I. Osipkov. Spamming botnets: Signatures and characteristics. In *SIGCOMM*, 2008.
- [28] H.-C. Yang, A. Dasdan, R.-L. Hsiao, and D. S. Parker. Map-Reduce-Merge: Simplified relational data processing on large clusters. In *ACM SIGMOD*, 2007.
- [29] Y. Yu, M. Isard, D. Fetterly, M. Budiu, U. Erlingsson, P. K. Gunda, and J. Currey. DryadLINQ: A system for general-purpose distributed data-parallel computing using a high-level language. In *OSDI*, 2008.